

The Meta Distribution of the SIR in Joint Communication and Sensing Networks

Kun Ma^{*}, Chenyuan Feng[†], Giovanni Geraci[‡], and Howard H. Yang^{*}

^{*} ZJU-UIUC Institute, Zhejiang University, Haining, China

[†] Department of Communication, EURECOM, France

[‡] Telefónica Research and Universitat Pompeu Fabra, Barcelona, Spain

Abstract—In this paper, we introduce a novel mathematical framework for assessing the performance of joint communication and sensing (JCAS) in wireless networks, employing stochastic geometry as an analytical tool. We focus on deriving the meta distribution of the signal-to-interference ratio (SIR) for JCAS networks. This approach enables a fine-grained quantification of individual user or radar performance intrinsic to these networks. Our work involves the modeling of JCAS networks and the derivation of exact mathematical expressions for the JCAS SIR meta distribution. Recognizing the computational complexity of these expressions, we also present practical, tight approximations. Through simulations, we validate both our exact and approximated theoretical analysis and illustrate how the JCAS SIR meta distribution varies with the network deployment density.

I. INTRODUCTION

One of the envisioned features of sixth generation (6G) mobile networks is the synergy between wireless communications and sensing [1]–[4]. Joint communication and sensing (JCAS) paves the way for diverse applications, such as indoor localization, autonomous aircraft, and extended reality [5]–[7], while also presenting a challenge in efficiently sharing the spectrum. To address this, a detailed analysis of the underlying trade-offs is necessary, with well-defined performance metrics to gauge the network’s effectiveness.

Stochastic geometry emerges as a robust analytical framework for this task, offering theoretical models to characterize network-wide performance. For instance, time-sharing networks were explored in [8], detailing their radar detection range, false alarm rates, and communication success probabilities. Other studies have focused on the energy and spectrum efficiency in base station (BS) deployments [9] and the extension of coverage probability and ergodic capacity concepts to radar settings [10]. Notably, JCAS techniques are also crucial in vehicular networks, with studies investigating the detection range in spectrum-sharing scenarios and the impact

K. Ma and H. H. Yang were supported by the National Natural Science Foundation of China under Grant 62201504, by the Zhejiang Provincial Natural Science Foundation of China under Grant LGJ22F010001, and by the Zhejiang Lab Open Research Project (No. K2022PD0AB05). C. Feng was supported by the French Beyond5G project. G. Geraci was supported by the Spanish Research Agency grants PID2021-123999OB-I00 and CEX2021-001195-M, by the UPF-Fractus Chair, and by the Spanish Ministry of Economic Affairs and Digital Transformation and the European Union NextGenerationEU through the UNICO 5G I+D SORUS project.

of interference on road obstacle detection and communication [11], [12].

Despite these advancements, a gap remains in understanding the individual performance of users or radars within a JCAS network. Existing studies have primarily concentrated on the coverage probability, a geographic average that only provides information about the expected JCAS performance across all network deployments, overlooking the variability in user or radar experiences. For example, while one network realization may exhibit a wide range of success probabilities (e.g., 0.5 to 0.99), another might show a narrower range (e.g., 0.85 to 0.95), yet both could have the same spatial average.

In this paper, we employ a more fine-grained tool and analyze the performance of JCAS networks by deriving the meta distribution of the signal-to-interference ratio (SIR), a concept previously introduced in [13]. While the SIR meta distribution has been applied separately to either communication or radar detection scenarios [14]–[17], our work uniquely applies it to JCAS networks. Our contributions can be summarized as follows:

- We establish an analytical framework for modeling the JCAS network, based on which we derive exact mathematical expressions for the conditional JCAS coverage probability and (the complementary of) its distribution, namely, the SIR meta distribution.
- As the above exact expressions may require a considerable effort to be numerically evaluated, we also propose tight approximations based on practical assumptions.
- We validate both our exact and approximated analysis through simulations, and present numerical results to illustrate the behavior of the JCAS SIR meta distribution with respect to the network deployment density.

II. SYSTEM MODEL

A. Network Deployment

We consider the JCAS wireless network depicted in Fig. 1, consisting of multiple base stations (BSs), users (UEs), and sensed objects (SOs). The locations of the BSs, UEs, and SOs are modeled as three independent homogeneous Poisson point processes (PPPs), denoted by Φ_b , Φ_u and Φ_s with intensities of λ_b , λ_u , and λ_s , respectively. The BSs are in charge of sending information packets to UEs in the downlink;

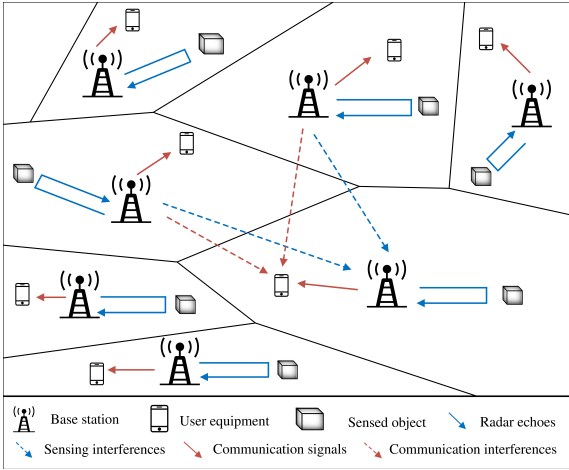


Fig. 1: Illustration of the JCAS network considered, with BSs simultaneously sending information packets to UEs and sensing waveforms to the SOs for which they receive radar echoes.

simultaneously, they send sensing waveforms to the SOs and receive echoes from them. We consider that communication and sensing functionalities are carried out via a shared multi-carrier waveform that is universally reused across the network; hence, the transmissions of different nodes will interfere with each other. All of the BSs are assumed to be active, and we have $\lambda_u \gg \lambda_b$ and $\lambda_s \gg \lambda_b$. We further assume that any pair of wireless transmission channels is subject to path loss, which obeys the power law, and Rayleigh fading, with the BSs transmitting at a fixed power P_{tx} . By utilizing the maximum average received power association policy, the UEs and SOs associate with the nearest BSs in space.

B. SIR Models

Based on Slivnyark's theorem [18], we can concentrate on a typical UE located at the origin. Let X_0 denote the location of the tagged BS (also referred to as the typical BS) of the typical UE and X_k denote the location of the k -th BS in the network. Then, the SIR received at the typical UE can be expressed as

$$\text{SIR}_c = \frac{h_0 \|X_0\|^{-\alpha}}{\sum_{k \neq 0} h_k \|X_k\|^{-\alpha}}, \quad (1)$$

where α is the path loss exponent, $h_k \sim \exp(1)$ stands for the channel fading from the k -th BS to the typical UE, and $\|\cdot\|$ denotes the Euclidean norm.

Similarly, we consider a monostatic sensing scenario where the BSs transmit the sensing waveforms and listen to the echo of the SOs. Without loss of generality, we place the typical SO at the origin [10]. As such, the signal strength of the radar echo measured at the typical BS is given by [19]

$$S_s = \frac{P_{tx} G_t G_r \lambda_w^2 \sigma_{cs} \|X_0\|^{-2\alpha}}{(4\pi)^3} = A \frac{\sigma_{cs}}{4\pi} \|X_0\|^{-2\alpha}, \quad (2)$$

where G_t and G_r denote the antenna gains of transmission and reception in the sensing stage, respectively, λ_w is the carrier wavelength, $\sigma_{cs} \sim \exp(1)$ represents the radar cross-section, which can be modeled as a random variable that

follows the exponential distribution with unit mean [20], and $A = PG_t G_r (\lambda_w / 4\pi)^2$.

Since sensing employs the same carrier as communication, the interference accumulated at the typical BS from all other BSs can be expressed as

$$I_s = \sum_{k \neq 0} A \tilde{h}_k \|X_k - X_0\|^{-\alpha} \quad (3)$$

By analogy with the communication scenario, the sensing SIR at the average BS can be written as follows

$$\text{SIR}_s = \frac{S_s}{I_s} = \frac{\frac{\sigma_{cs}}{4\pi} \|X_0\|^{-2\alpha}}{\sum_{k \neq 0} \tilde{h}_k \|X_k - X_0\|^{-\alpha}}. \quad (4)$$

We note that while SIR_c is an actual SIR, SIR_s is a conceptual one, constructed as a proxy for the BS's efficacy in estimating the SO's parameter of interest.¹ Based on these SIR models, we can establish suitable metrics to assess the JCAS network performance.

C. Performance Metric

The probability that SIR_c surpasses a decoding threshold θ_c is known as the coverage probability, a widely used metric to evaluate link performance in cellular networks. This metric provides information about the fraction of UEs in the network that achieves a SIR at least at the level of θ_c . The sensing performance can be defined in a similar manner. The estimation rate, which is the mutual information between the radar return and the parameter of interest divided by coherent processing interval, can be used to characterize the quality of the sensing, with upper and lower bounds determined by logarithmic functions of SIR_s [10]. Hence, the sensing accuracy can be captured using a measure based on the distribution of SIR_s . For instance, one could consider the sensing coverage probability, defined as the probability of SIR_s surpassing a predetermined threshold θ_s and reflecting the average portion of the SOs whose SIR reaches θ_s .

Since the coverage probabilities only provide information about the average JCAS performance across all network deployments, in this paper, we leverage the notion of conditional coverage probability and meta SIR distribution [13]–[15] to obtain a fine-grained perspective of the network performance. Specifically, given the point process Φ_b , we define the *conditional JCAS coverage probability* as follows:

$$P(\theta_c, \theta_s) = \mathbb{P}(\text{SIR}_c > \theta_c, \text{SIR}_s > \theta_s \mid \Phi_b). \quad (5)$$

We note that $P(\theta_c, \theta_s)$ is still a random variable, since while channel fading is averaged out, the randomness stemming from Φ_b remains.² We then define the complementary cumulative distribution function (CCDF) of $P(\theta_c, \theta_s)$ as the *JCAS SIR meta distribution*, given by

$$F(\theta_c, \theta_s, x) = \mathbb{P}(P(\theta_c, \theta_s) > x), \quad x \in [0, 1]. \quad (6)$$

¹In the following, for the sake of readability, we neglect the constant multiplier $\frac{1}{4\pi}$ in (4) as it can be embedded into the decoding threshold.

²The conventional coverage probability can be obtained by taking the expectation of $P(\theta_c, \theta_s)$ with respect to Φ_b , thereby disregarding the dependence of the JCAS performance on the network realization Φ_b .

The meta distribution $F(\theta_c, \theta_s, x)$ quantifies the probability that the UEs and SOs in the network can attain SIR_c of θ_c and SIR_s of θ_s , with a link reliability (i.e., probability) of at least x .

III. ANALYSIS OF JCAS SIR META DISTRIBUTION

This section details the steps followed to derive analytical expressions for the quantity in (6).

A. Exact Analysis of the JCAS SIR Meta Distribution

Conditional JCAS coverage probability: We begin by deriving the conditional JCAS coverage probability $P(\theta_c, \theta_s)$ by averaging out the randomness in channel fading. The quantity $P(\theta_c, \theta_s)$ represents the probability that, given a network realization Φ_b , the effect of channel fading results in communication and sensing SIRs exceeding θ_c and θ_s , respectively.

Lemma 1: *Conditioned on the point process Φ_b , the JCAS coverage probability is given by*

$$P(\theta_c, \theta_s) = \prod_{k \neq 0} \frac{1}{\left(1 + \theta_c \frac{\|X_0\|^\alpha}{\|X_k\|^\alpha}\right) \left(1 + \theta_s \frac{\|X_0\|^{2\alpha}}{\|X_k - X_0\|^\alpha}\right)}. \quad (7)$$

Proof: Using (1) and (4), we can calculate the conditional JCAS coverage probability as

$$\begin{aligned} P(\theta_c, \theta_s) &= \mathbb{P}(\text{SIR}_c > \theta_c, \text{SIR}_s > \theta_s \mid \Phi_b) \\ &\stackrel{(a)}{=} \mathbb{P}\left(h_0 > \theta_c \|X_0\|^\alpha \sum_{k \neq 0} h_k \|X_k\|^{-\alpha} \mid \Phi_b\right) \\ &\quad \times \mathbb{P}\left(\sigma_{cs} > \theta_s \|X_0\|^{2\alpha} \sum_{k \neq 0} \tilde{h}_k \|X_k - X_0\|^{-\alpha} \mid \Phi_b\right) \\ &\stackrel{(b)}{=} \mathbb{E}\left\{\exp\left(-\theta_c \|X_0\|^\alpha \sum_{k \neq 0} h_k \|X_k\|^{-\alpha}\right)\right\} \\ &\quad \times \mathbb{E}\left\{\exp\left(-\theta_s \|X_0\|^{2\alpha} \sum_{k \neq 0} \tilde{h}_k \|X_k - X_0\|^{-\alpha}\right)\right\} \\ &\stackrel{(c)}{=} \prod_{k \neq 0} \frac{1}{\left(1 + \theta_c \frac{\|X_0\|^\alpha}{\|X_k\|^\alpha}\right) \left(1 + \theta_s \frac{\|X_0\|^{2\alpha}}{\|X_k - X_0\|^\alpha}\right)}, \end{aligned} \quad (8)$$

where (a) holds since channel fading realizations are mutually independent, while (b) and (c) follow from noticing that h_0 and σ_{cs} obey exponential distributions. \square

JCAS SIR meta distribution: Next, we derive the JCAS SIR meta distribution, defined as the CCDF of $P(\theta_c, \theta_s)$.

Theorem 1: *The meta distribution of the SIR in the JCAS network under consideration is given by*

$$F(\theta_c, \theta_s, x) = \frac{1}{2} - \frac{1}{\pi} \int_0^\infty \text{Im}\left\{x^{-j\omega} M_{j\omega}\right\} \frac{d\omega}{\omega}, \quad (9)$$

where $j = \sqrt{-1}$, $\text{Im}\{\cdot\}$ denotes the imaginary part of the input variable, and M_b is the b -th moment of $P(\theta_c, \theta_s)$, given by

$$M_b = \int_0^\infty 2\pi \lambda_b r_0 \exp(-\lambda_b \pi r_0^2 - \lambda_b F_b(r_0)) dr_0, \quad (10)$$

with

$$\begin{aligned} F_b(r_0) &= - \sum_{t=1}^\infty \binom{-b}{t} \sum_{i_1+i_2+i_3=t} \binom{t}{i_1, i_2, i_3} \theta_c^{i_1+i_3} \\ &\quad \times \theta_s^{i_2+i_3} \int_0^{2\pi} \int_1^\infty \frac{r_0^{(i_2+i_3)\alpha+2} v^{1-(i_1+i_3)\alpha} dv d\theta}{(v^2+1-2v\cos(\theta))^{(i_2+i_3)\alpha/2}}. \end{aligned} \quad (11)$$

Proof: Please refer to Appendix A. \square

JCAS coverage probability: As a byproduct, we can obtain the JCAS coverage probability [10] by computing the first moment of (7) with respect to Φ_b , denoted as $\bar{P}(\theta_c, \theta_s) = \mathbb{E}\{P(\theta_c, \theta_s)\}$ and characterized as follows.

Corollary 1: *The JCAS coverage probability is given by*

$$\bar{P}(\theta_c, \theta_s) = \int_0^\infty 2\pi \lambda_b r_0 \exp(-\lambda_b \pi r_0^2 - \lambda_b F_c(r_0)) dr_0, \quad (12)$$

in which

$$F_c(r_0) = \int_0^{2\pi} \int_1^\infty \left[1 - \frac{(v^2+1-2v\cos\theta)^{\frac{\alpha}{2}} v^\alpha}{((v^2+1-2v\cos\theta)^{\frac{\alpha}{2}} + \theta_s r_0^\alpha)(v^\alpha + \theta_c)}\right] r_0^2 v dv d\theta. \quad (13)$$

Proof: Equation (12) follows by setting $b = 1$ in (10). \square

B. Approximation of the JCAS SIR Meta Distribution

Approximated conditional JCAS coverage probability: While Theorem 1 provides an exact analytical expression for the JCAS SIR meta distribution, evaluating it can be computationally expensive due to the infinite summation in (11). To obtain a simplified expression, we approximate the conditional JCAS coverage probability in (7) via a beta distribution [13] by matching the first and second moments, M_1 and M_2 .

Approximated JCAS SIR meta distribution: The JCAS SIR meta distribution (9) can then be approximated as

$$F(\theta_c, \theta_s, x) \approx 1 - I_v\left(\frac{\beta\mu}{1-\mu}, \beta\right), \quad v \in [0, 1], \quad (14)$$

where $I_v(x, y) = \int_0^{1-v} z^{x-1} (1-z)^{y-1} dz / B(x, y)$ is the regularized incomplete beta function, in which $B(\cdot, \cdot)$ denotes the beta function, and $\mu = M_1$ and $\beta = \frac{(M_1 - M_2)(1 - M_1)}{M_2 - M_1^2}$. Since the above requires computing the first two moments, and since the exact expression of the b -th moment in (10) contains multiple nested integrals, we adopt the following approximation, which treats communication and sensing independently and whose accuracy will be validated in Fig. 2.

Corollary 2: *The b -th moment of $P(\theta_c, \theta_s)$ can be approximated as*

$$M_b \approx \int_0^\infty 2\pi \lambda_b r_0 \exp(-\lambda_b \pi r_0^2 - \lambda_b (F_b^c + F_b^s(r_0))) dr_0, \quad (15)$$

where

$$F_b^c = \pi r_0^2 C_1(b, \theta_c, \delta), \quad (16)$$

$$F_b^s(r_0) = 4\pi r_0^2 C_1\left(b, \theta_s \left(\frac{r_0}{2}\right)^{\frac{2}{3}}, \delta\right) + 2\pi r_0^2 C_2\left(b, \theta_s \left(\frac{r_0}{2}\right)^{\frac{2}{3}}, \delta\right)$$

$$+ 4r_0^2 \sum_{n=0}^\infty \frac{\Gamma(n + \frac{1}{2})}{\Gamma(\frac{1}{2})n!(1+2n)} C_2\left(b, \theta_s \left(\frac{r_0}{2}\right)^{\frac{2}{3}}, \delta \left(n + \frac{3}{2}\right)\right), \quad (17)$$

in which $\delta = 2/\alpha$, $\Gamma(\cdot)$ is the gamma function, and

$$C_1(x, y, z) = {}_2F_1(x, -z; 1 - z; y) - 1, \quad (18)$$

$$C_2(x, y, z) = 1 - {}_2F_1\left(x, x+z; x+z+1; -\frac{1}{y}\right) \times \frac{z}{y^x(x+z)} \quad (19)$$

whereas ${}_2F_1(\cdot, \cdot; \cdot, \cdot)$ represents the Gaussian hyper-geometric function.

Proof: Please refer to Appendix B. \square

A simpler approximated expression for the SIR meta distribution can then be obtained by replacing (9) with (14) and adopting (15) in place of (10) for the moments computation.

Approximated JSAC coverage probability: Finally, the JCAS coverage probability can be approximated as

$$\bar{P}(\theta_c, \theta_s) \approx \bar{P}_c(\theta_c) \times \bar{P}_s(\theta_s), \quad (20)$$

in which

$$\bar{P}_c(\theta_c) = \frac{1}{{}_2F_1(1, -\delta; 1 - \delta; -\theta_c)}, \quad (21)$$

$$\bar{P}_s(\theta_s) = \int_0^\infty 2\pi\lambda_b r_0 \exp(-\lambda_b(\pi r_0^2 + F_1^s(r_0))) dr_0, \quad (22)$$

where $F_1^s(\cdot)$ can be calculated by setting $b = 1$ in (17). Specifically, equation (20) follows by treating the sensing and communication functionalities as independent, (21) from [21], and (22) from (30) by setting $b = 1$ and de-conditioning on the distance r_0 between the SO and its serving BS.

By comparing (21) to (22), we note that while the communication coverage probability does not depend on the BS density λ_b —a known result for the system model adopted in this paper—the sensing coverage probability does.

IV. NUMERICAL RESULTS

We now provide numerical results to validate our analysis and evaluate how the JCAS SIR meta distribution is affected by the SIR thresholds and by the BS density. We generate 100 PPP realizations for the locations of BSs, UEs, and SOs. Within the Voronoi cell formed by the BSs, UEs and SOs are situated in a square area measuring 1,000 m in width on each side. Once constructed, the topology remains unchanged, but the fading realizations of communications and sensing across each link are recalculated across 1,000 time periods. Then, we collect the statistics of communications and sensing to compute the conditional JSAC coverage probability of each realization. We adopt the following parameters unless otherwise noted: $\alpha = 4$, $\lambda_b = 10^{-4} \text{ m}^{-2}$, and $\lambda_u = \lambda_s = 10^{-3} \text{ m}^{-2}$.

Fig. 2 compares the simulated CCDF of the conditional JCAS coverage probability (black circles) to the exact analysis in Theorem 1 (red solid) and the approximation obtained using Corollary 2 (blue dashed), under various pairs of communication and sensing thresholds. The close match of all three validates both our exact mathematical derivations in Theorem 1 and the proposed approximation based on Corollary 2.

The JCAS SIR meta distribution in Fig. 2 provides a fine-grained evaluation of the network performance in terms of both communication and sensing. For instance, the plot shows that for $\theta_c = \theta_s = 0 \text{ dB}$ and $\theta_c = \theta_s = 10 \text{ dB}$, respectively,

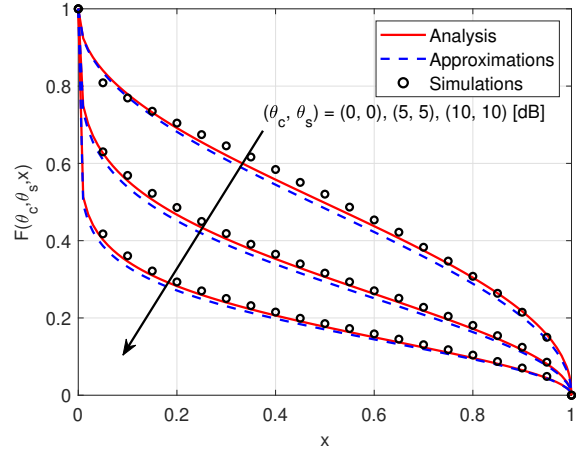


Fig. 2: SIR meta distribution via exact analysis (Theorem 1), approximated analysis (Corollary 2), and simulations, as a function of the reliability threshold (x-axis) and for different SIR thresholds (θ_c, θ_s) .

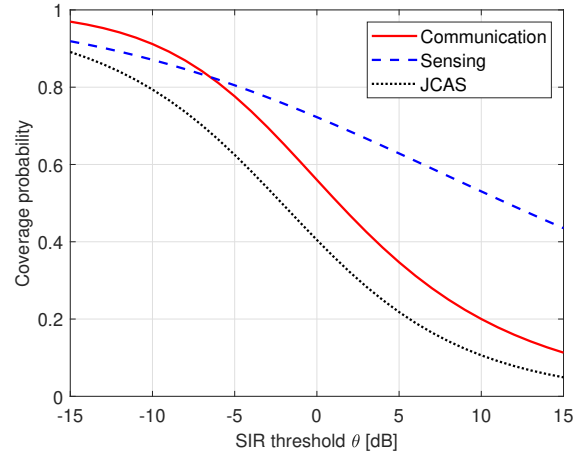


Fig. 3: Coverage probability of communication only, sensing only, and JCAS versus SIR threshold $\theta_c = \theta_s = \theta$.

setting a reliability threshold of 0.8 on the x-axis corresponds to values of about 0.3 and 0.1 on the y-axis. This indicates that 30% of the BSs in this network can simultaneously achieve communication and sensing SIRs of at least 0 dB with an 80% reliability, but this fraction drops to 10% when both SIR thresholds are raised to 10 dB.

In Fig. 3, we plot the coverage probabilities of communication only, sensing only, and JCAS, vs. the decoding thresholds according to Corollary 2. While for convenience of plotting the two SIR thresholds are equally set as $\theta_c = \theta_s$, our framework allows to compute the coverage probability for any combination of values. Fig. 3 shows that compared to sensing, the coverage probability of communication is more sensitive to changes in the SIR threshold. This indicates that the sensing performance exhibits more variability across SOs than the communication performance does across UEs.

Fig. 4 depicts the sensing coverage probability as a func-

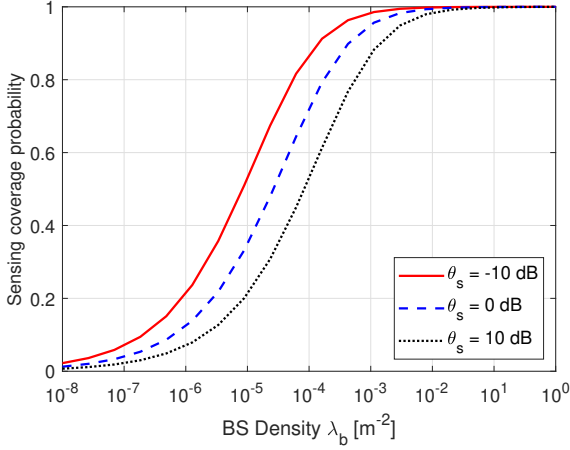


Fig. 4: Sensing coverage probability versus BS deployment density λ_b under different decoding thresholds θ_s .

tion of the BS deployment density for three values of the SIR threshold. In line with the findings in [10], the figure shows that the sensing coverage probability increases with the BS deployment density. This is in contrast to what occurs to communications under the adopted single-slope pathloss assumption, where the coverage probability is independent of the BS density, as captured in (21).

V. CONCLUSION

In this paper, we developed a framework to assess the performance of JCAS in wireless networks, utilizing stochastic geometry as a key analytical apparatus. Our approach involved deriving mathematical expressions for the conditional JCAS coverage probability and its distribution, known as the SIR meta distribution. Given the computational complexity of these expressions, we also presented practical, tight approximations for simpler numerical evaluations. Our theoretical models, validated through simulations, capture the impact of network deployment density on the JCAS SIR performance. Unlike previous studies, our analysis allows to quantify individual user or radar performance within network realizations.

While this work primarily focused on the impact of network deployment density on the JCAS SIR meta distribution, we note that this distribution is also influenced by the propagation environment model and the specific deployment scenario. Future research directions include examining JCAS performance for channels with line-of-sight (LoS) and non-LoS state transitions, and incorporating a minimum BS inter-site distance. Exploring dynamics in the temporal domain, such as data traffic for communication [22] and status updates for sensing [23], is another avenue for further investigation.

APPENDIX A: PROOF OF THEOREM 1

The b -th moment of $P(\theta_c, \theta_s)$ can be expressed as:

$$M_b = \mathbb{E} \left\{ \prod_{k \neq 0} \left(\frac{1}{\left(1 + \theta_c \frac{\|X_0\|^\alpha}{\|X_k\|^\alpha}\right) \left(1 + \theta_s \frac{\|X_0\|^{2\alpha}}{\|X_k - X_0\|^\alpha}\right)} \right)^b \right\}$$

$$\stackrel{(a)}{=} \mathbb{E} \left\{ \mathbb{E}_{X_0} \left\{ \exp \left(-\lambda_b F_b(\|X_0\|) \right) \right\} \right\}, \quad (23)$$

where (a) follows by leveraging the probability generating function (PGFL) of PPP and conditioning on the location of the serving BS X_0 .

By writing X_0 in polar coordinates as $X_0 = (r_0, \theta_0)$, the analytical expression of $F_b(r_0)$ can be derived as

$$\begin{aligned} F_b(r_0) &= \int_{\mathbb{R}^2/B(0,r_0)} \left[1 - \frac{1}{\left(1 + \theta_c \frac{r_0^\alpha}{\|\mathbf{x}\|^\alpha}\right)^b \left(1 + \theta_s \frac{r_0^{2\alpha}}{\|\mathbf{x} - X_0\|^\alpha}\right)^b} \right] d\mathbf{x} \\ &\stackrel{(b)}{=} - \sum_{i=1}^{\infty} \binom{-b}{i} \sum_{i_1+i_2+i_3=i} \binom{i}{i_1, i_2, i_3} \theta_c^{i_1+i_3} \\ &\quad \times \theta_s^{i_2+i_3} \int_{\mathbb{R}^2/B(0,r_0)} \frac{r_0^{i_1+2i_2+3i_3}}{\left(\|\mathbf{x}\|^{i_1+i_3} \|\mathbf{x} - X_0\|^{i_2+i_3}\right)^b} d\mathbf{x} \\ &\stackrel{(c)}{=} - \sum_{i=1}^{\infty} \binom{-b}{i} \sum_{i_1+i_2+i_3=i} \binom{i}{i_1, i_2, i_3} r_0^{(i_1+2i_2+3i_3)\alpha} \\ &\quad \times \int_0^{2\pi} \int_{r_0}^{\infty} \frac{\theta_c^{i_1+i_3} \theta_s^{i_2+i_3} r^{1-(i_1+i_3)\alpha} dr d\theta}{(r^2 + r_0^2 - 2rr_0 \cos(\theta - \theta_0))^{(i_2+i_3)\alpha/2}} \\ &\stackrel{(d)}{=} - \sum_{i=1}^{\infty} \binom{-b}{i} \sum_{i_1+i_2+i_3=i} \binom{i}{i_1, i_2, i_3} r_0^{(i_2+i_3)\alpha+2} \\ &\quad \times \theta_c^{i_1+i_3} \theta_s^{i_2+i_3} \int_0^{2\pi} \int_1^{\infty} \frac{v^{1-(i_1+i_3)\alpha} dv d\theta}{(v^2 + 1 - 2v \cos \theta)^{(i_2+i_3)\alpha/2}}, \end{aligned} \quad (24)$$

where $B(0, r_0)$ denotes a disk centered at the origin with radius r_0 , (b) follows by applying the binomial expansion, i.e., $\binom{i}{i_1, i_2, i_3} = \frac{i!}{i_1! i_2! i_3!}$, indicating all sequences of non-negative integers that sum up to i , with i_1, i_2, i_3 representing the three different sequences; (c) holds due to the integration on the polar coordinates of $\mathbf{x} = (r, \theta)$, and (d) substituting $v = r/r_0$ and eliminating θ_0 because of periodicity. Substituting (24) into (23) and de-conditioning on r_0 , we obtain the expression of the b -th moment given in (10). The proof is concluded by invoking the Gil-Paleaz theorem [24] and then substituting (10) into (9).

APPENDIX B: PROOF OF COROLLARY 2

Assuming communication and sensing to be independent, the b -th moment can be approximated as

$$\begin{aligned} M_b &= \mathbb{E} \left\{ \prod_{k \neq 0} \left(\frac{1}{\left(1 + \theta_c \frac{\|X_0\|^\alpha}{\|X_k\|^\alpha}\right) \left(1 + \theta_s \frac{\|X_0\|^{2\alpha}}{\|X_k - X_0\|^\alpha}\right)} \right)^b \right\} \\ &\approx \mathbb{E}_{r_0} \left\{ \underbrace{\mathbb{E} \left\{ \prod_{k \neq 0} \left(\frac{1}{1 + \theta_c \frac{\|X_0\|^\alpha}{\|X_k\|^\alpha}} \right)^b \mid r_0 \right\}}_{M_{b|r_0}^c} \right. \\ &\quad \left. \times \mathbb{E} \left\{ \prod_{k \neq 0} \left(\frac{1}{1 + \theta_s \frac{\|X_0\|^{2\alpha}}{\|X_k - X_0\|^\alpha}} \right)^b \mid r_0 \right\} \right\} \end{aligned} \quad (25)$$

Then, one must determine the moment of the coverage probability for both sensing and communication, conditioned on the distance between the serving BS and the origin, $r_0 = \|X_0\|$, separately.

According to [25], the conditional moment of the communication coverage probability can be derived as

$$M_{b|r_0}^c = \exp\left(-\lambda_b \pi r_0^2 \left({}_2F_1(b, -\delta; 1 - \delta; -\theta_c) - 1\right)\right) \quad (26)$$

where the Gaussian hyper-geometric function ${}_2F_1(\cdot, \cdot; \cdot, \cdot)$ originates from the calculation of the integral in (27) [26, 3.194]. Since the proof will employ this type of integration several times, we use the following notations for convenience:

$$C_1(x, y, z) = z \int_0^1 \left(1 - \frac{1}{(1 + yu)^x}\right) u^{-z-1} du \\ = {}_2F_1(x, -z; 1 - z; y) - 1 \quad (27)$$

$$C_2(x, y, z) = z \int_1^\infty \left(1 - \frac{1}{(1 + yu)^x}\right) u^{-z-1} du \\ = 1 - \left(\frac{z}{y^x(x+z)}\right) {}_2F_1(x, x+z; x+z+1; -\frac{1}{y}) \quad (28)$$

Lemma 2 of [10] states that the point process of the distance of interfering BSs with regard to serving BS conditioned on r_0 is a PPP on \mathbb{R}_+ with the following intensity function, provided as $\Pi_B^0 = \{\|X_k - X_0\| : X_k \in \Phi_{B^c}^{r_0}\}$:

$$\lambda_b^0(r; r_0) = 2\lambda_b r (\pi - \arccos(\frac{r}{2r_0})) \mathbb{1}\{r \leq 2r_0\}. \quad (29)$$

Then via the PGFL of PPP, the conditional moment of the sensing coverage probability can be derived as

$$M_{b|r_0}^s = \exp\left(-\int_{\mathbb{R}^2} \left[1 - \frac{1}{(1 + \theta_s r_0^{2\alpha} r^{-\alpha})^b}\right] \lambda_b^0(r; r_0) dr\right) \\ \stackrel{(a)}{=} \exp\left(-4\lambda_b \pi r_0^2 \delta \int_0^1 \left(1 - \frac{1}{(1 + \theta_s (\frac{r_0}{2})^{\frac{2}{\alpha}} v)^b}\right) v^{-\delta-1} dv \right. \\ \left. - 2\lambda_b \pi r_0^2 \delta \int_1^\infty \left(1 - \frac{1}{(1 + \theta_s (\frac{r_0}{2})^{\frac{2}{\alpha}} v)^b}\right) v^{-\delta-1} dv \right. \\ \left. - 4\lambda_b r_0^2 \delta \sum_{n=0}^\infty \frac{\Gamma(n + \frac{1}{2})}{\Gamma(\frac{1}{2}) n! (1 + 2n)} \right. \\ \left. \times \int_1^\infty \left(1 - \frac{1}{(1 + \theta_s (\frac{r_0}{2})^{\frac{2}{\alpha}} v)^b}\right) v^{-\delta(n + \frac{3}{2})-1} dv\right) \\ \stackrel{(b)}{=} \exp(-\lambda_b F_b^s(r_0)) \quad (30)$$

where step (a) follows by the substitution of $v = (\frac{2r_0}{r})^\alpha$ and the Taylor expansion of $\arcsin(x)$, step (b) shows the calculation of the integration with (27) and (28) and $F_b^s(r_0)$ is defined as (17). The proof is completed by de-conditioning on r_0 and substituting (30) and (26) in (25).

REFERENCES

- [1] F. Tariq, M. R. Khandaker, K.-K. Wong, M. A. Imran, M. Bennis, and M. Debbah, "A speculative study on 6G," *IEEE Wireless Commun.*, vol. 27, no. 4, pp. 118–125, Aug. 2020.
- [2] E. Oughton, G. Geraci, M. Polese, and V. Shah, "Prospective evaluation of next generation wireless broadband technologies: 6G versus Wi-Fi 7/8," Available at SSRN: <https://ssrn.com/abstract=4528119>, 2023.
- [3] S. Dang, O. Amin, B. Shihada, and M.-S. Alouini, "What should 6G be?" *Nature Electronics*, vol. 3, no. 1, pp. 20–29, 2020.
- [4] T. Wild, V. Braun, and H. Viswanathan, "Joint design of communication and sensing for beyond 5G and 6G systems," *IEEE Access*, vol. 9, pp. 30 845–30 857, 2021.
- [5] C. De Lima, D. Belot, R. Berkvens, A. Bourdoux, D. Dardari, M. Guillaud, M. Isomursu, E.-S. Lohan, Y. Miao, A. N. Barreto *et al.*, "Convergent communication, sensing and localization in 6G systems: An overview of technologies, opportunities and challenges," *IEEE Access*, vol. 9, pp. 26 902–26 925, 2021.
- [6] F. Liu, C. Masouros, A. P. Petropulu, H. Griffiths, and L. Hanzo, "Joint radar and communication design: Applications, state-of-the-art, and the road ahead," *IEEE Trans. Commun.*, vol. 68, no. 6, pp. 3834–3862, 2020.
- [7] J. A. Zhang, M. L. Rahman, K. Wu, X. Huang, Y. J. Guo, S. Chen, and J. Yuan, "Enabling joint communication and radar sensing in mobile networks—A survey," *IEEE Commun. Surv. Tutor.*, vol. 24, no. 1, pp. 306–345, 2021.
- [8] P. Ren, A. Munari, and M. Petrova, "Performance analysis of a time-sharing joint radar-communications network," in *2020 International Conference on Computing, Networking and Communications (ICNC)*. IEEE, 2020, pp. 908–913.
- [9] A. Salem, C. Masouros, F. Liu, and D. López-Pérez, "Rethinking dense cells for integrated sensing and communications: A stochastic geometric view," Available as *ArXiv:2212.12942*, 2022.
- [10] N. R. Olson, J. G. Andrews, and R. W. Heath Jr, "Coverage and capacity of joint communication and sensing in wireless networks," Available as *ArXiv:2210.02289*, 2022.
- [11] D. Ghazlani, A. Omri, S. Bouallegue, H. Chamkhia, and R. Bouallegue, "Stochastic geometry-based analysis of joint radar and communication-enabled cooperative detection systems," in *Proc. IEEE WiMob*, 2021, pp. 325–330.
- [12] H. Ma, Z. Wei, Z. Li, F. Ning, X. Chen, and Z. Feng, "Performance of cooperative detection in joint communication-sensing vehicular network: A data analytic and stochastic geometry approach," *IEEE Trans. Veh. Technol.*, vol. 72, no. 3, pp. 3848–3863, 2022.
- [13] M. Haenggi, "The meta distribution of the SIR in Poisson bipolar and cellular networks," *IEEE Trans. Wireless Commun.*, vol. 15, no. 4, pp. 2577–2589, Apr. 2016.
- [14] M. Haenggi, "Meta distributions—Part 1: Definition and examples," *IEEE Commun. Lett.*, vol. 25, no. 7, pp. 2089–2093, Jul. 2021.
- [15] M. Haenggi, "Meta distributions—Part 2: Properties and interpretations," *IEEE Commun. Lett.*, vol. 25, no. 7, pp. 2094–2098, Jul. 2021.
- [16] G. Ghatak, S. S. Kalamkar, and Y. Gupta, "Radar detection in vehicular networks: Fine-grained analysis and optimal channel access," *IEEE Trans. Veh. Technol.*, vol. 71, no. 6, pp. 6671–6681, 2022.
- [17] S. S. Ram, S. Singhal, and G. Ghatak, "Optimization of network throughput of joint radar communication system using stochastic geometry," *Frontiers in Signal Processing*, vol. 2, p. 835743, 2022.
- [18] A. Baddeley, P. Gregori, J. Mateu, R. Stoica, and D. Stoyan, *Case Studies in Spatial Point Process Modeling. Lecture Notes in Statistics*. Springer, 2006.
- [19] M. A. Richards, *Fundamentals of radar signal processing*. Mcgraw-hill New York, 2005, vol. 1.
- [20] D. Shnidman, "Expanded swerling target models," *IEEE Trans. Aerosp. Electron. Syst.*, vol. 39, no. 3, pp. 1059–1069, 2003.
- [21] J. G. Andrews, F. Baccelli, and R. K. Ganti, "A tractable approach to coverage and rate in cellular networks," *IEEE Trans. Commun.*, vol. 59, no. 11, pp. 3122–3134, Nov. 2011.
- [22] H. H. Yang, T. Q. S. Quek, and H. V. Poor, "A unified framework for SINR analysis in Poisson networks with traffic dynamics," *IEEE Trans. Commun.*, vol. 69, no. 1, pp. 326–339, Jan. 2021.
- [23] H. H. Yang, C. Xu, X. Wang, D. Feng, and T. Q. S. Quek, "Understanding age of information in large-scale wireless networks," *IEEE Trans. Wireless Commun.*, vol. 20, no. 5, pp. 3196–3210, May 2021.
- [24] J. Gil-Pelaez, "Note on the inversion theorem," *Biometrika*, vol. 38, no. 3–4, pp. 481–482, Dec. 1951.
- [25] R. K. Ganti and M. Haenggi, "Asymptotics and approximation of the SIR distribution in general cellular networks," *IEEE Trans. Wireless Commun.*, vol. 15, no. 3, pp. 2130–2143, 2015.
- [26] I. S. Gradshteyn and I. M. Ryzhik, *Table of Integrals, Series, and Products*. Academic Press, 2007.